Journal of Hydrology 590 (2020) 125518

Contents lists available at ScienceDirect

Journal of Hydrology

journal homepage: www.elsevier.com/locate/jhydrol

Research papers

Data fusion of citizen-generated smartphone discharge measurements in Tunisia

Raed Fehri[a,*], Patrick Bogaert[a], Slaheddine Khlifi[b], Marnik Vanclooster[a]

[a] Université catholique de Louvain, Earth and Life Institute (ELI), Croix du Sud 2, 1348 Louvain-La-Neuve, Belgium

[b] Ecole Supérieure des Ingénieurs de Medjez el Bab (ESIM), UR-Gestion Durable des Ressources en Eau et en Sol, P5, 9070, Tunisia

A R T I C L E I N F O

This manuscript was handled by G. Syme, Editor-in-Chief

Keywords:
Citizen science
Discharge measurement
Data fusion
Smartphone application
Medjerda river

A B S T R A C T

Water resources management techniques have been evolving over the years, introducing new ways of monitoring and collecting data that improve both the quality and quantity of water-related information. Among them, Citizen Science (CS) has been introduced in the field of environmental monitoring as a novel approach that involves a direct collaboration between citizens, scientists and local authorities.

In Tunisia, the lack of reliable hydrological data about rivers' discharge remains a major issue, despite the recent governmental efforts to reinforce the existing official monitoring systems. In this study, we show how this problem can be efficiently addressed using a CS methodology. Citizens at two locations in Tunisia (Slouguia and Medjez-N5) have monitored discharge of the Medjerda river (the most important water resource in the country) using a mobile phone application for a series of hydrological events. Using a Best Linear Unbiased Predictor (BLUP) as a data fusion procedure for combining the various CS measurements, the results show that predicted discharge at both locations is in very good agreement with the reference data collected for the same hydrological events. Based on a variance decomposition, this approach allows us as well to properly assess the respective part of the random errors that are related to the citizens and measuring devices.

It is concluded that CS-based discharge data collection is a promising cost-effective way for obtaining reliable and numerous measurements. The monitoring approach based on the use of a mobile phone application is thus quite valuable for complementing the existing Tunisian monitoring system, as well as for empowering local communities. Furthermore, this approach can be applied at larger scales in the country by involving more citizens and adding other sites, which should support the national efforts for better and smarter water resources management.

1. Introduction

Efficient strategies of water resources management require the availability of reliable hydrometric quantities such as rivers' discharge and rainfall. These data are needed to assess and model catchments' hydrological behavior over time. Nevertheless, in many regions of the world, the availability of water-related data (especially discharge) is still a major concern, especially in Africa (Hannah et al., 2011). One of the main reasons are the high acquisition and maintenance costs of the traditional discharge measurement methods (which are relying on advanced sensors like pressure transducers); costly, dangerous, and time-consuming site management (e.g., improvement of cross-sections); and expert knowledge (Davids et al., 2019). Within the African regions, Tunisia is no exception with respect to this issue (Sellami et al., 2013; Fehri et al., 2019). Despite the recent governmental efforts to boost the availability and accuracy of relevant hydrological data, several issues persist. The access to data is still not publically available and is limited to specific governmental institutions, which represents a major disadvantage for local groups and stakeholders. In addition, current official discharge monitoring networks are not spatially dense and suffer from data gaps, leading to scarce and incomplete time series and consequently poor quality databases (Fehri et al., 2020).

By the light of these challenges and accounting for the growing demand of water-related data, alternative cost-effective discharge monitoring solutions have been developed thanks to the availability of new smart sensing technologies, offering novel approaches that can be used for improving the availability and reliability of hydrometric information (Paul et al., 2018). As an example, discharge estimation using remote sensing techniques have been successfully used in several studies (Tarpanelli et al., 2011; Brakenridge et al., 2007; Van Dijk et al.,

* Corresponding author.
E-mail address: raed.fehri@uclouvain.be (R. Fehri).

https://doi.org/10.1016/j.jhydrol.2020.125518
Received 16 March 2020; Received in revised form 4 September 2020; Accepted 5 September 2020
Available online 13 September 2020

2016). However, applications of remote sensing-based technology in the context of small streams remain problematic (Tauro et al., 2018) and motivate the use of ground-based indirect discharge measurements. In this context, image and video analysis techniques such as Particle Tracking Velocimetry (PTV), Particle Image Velocimetry (PIV), Surface Structure Imaging Velocimetry (SSIV), and Large-Scale Particle Image Velocimetry (LSPIV) are being widely used for extracting water level and surface flow velocity using simple and inexpensive equipment such as fixed cameras and smartphones (Nezu and Sanjou, 2011; Lüthi et al., 2018; Kantoush et al., 2011). Indeed, camera-based discharge measurements become more available and can be used in floods assessment and rating curve establishment (Dramais et al., 2011; Le Boursicaud et al., 2016). In parallel, over the last decade, the involvement of citizen scientists through Citizen Science (CS) initiatives has been emerging. It can potentially help filling the existing hydrological data gap by generating additional hydrologic information, including discharge (Fujita et al., 2013; Le Coz et al., 2016; See, 2019; Davids et al., 2019; Fehri et al., 2020).

Dickinson et al. (2012) define CS as the engagement of non-professionals in authentic scientific research, while Buytaert et al. (2014) described it as the participation of the general public (i.e., non-scientists) in the generation of new scientific knowledge. Fehri et al. (2020) define CS as a complex process built on civic engagement into science, environmental monitoring and capacity building. Nevertheless, the definition of CS depends mainly on the specific goals of the project, i.e. whether it aims at engaging volunteers for data collection (which is known as crowdsourcing) or empowering and including citizens in knowledge generation activities, training, and capacity building, which is considered as a more advanced form of CS (Pocock et al., 2019). In addition, Roy et al. (2012) provide a classification of CS based on the context of the projects. Three main approaches are recognized: contributory projects (entirely designed by scientists while citizens are mainly participating in data collection), collaborative projects (also designed by scientists while citizens are more involved in the scientific process such as collecting and analyzing data), and co-created projects (designed in collaboration between scientists and citizens as both work together in partnership). Whatever the exact definition one is using, participation and empowerment of the general public at any level within a region or a country suggests that everyday citizens have the potential to deliver timely and cost-effective alternatives to traditional data collection (Walker et al., 2016). In this sense, CS is helpful for improving integrated water resources management, thus contributing to the implementation of the water-related Sustainable Development Goal (SDG-6) (Fritz et al., 2019).

Despite the rapid expansion of CS and the activity of community-based monitoring, considerable attention needs to be paid to the quality of CS-based data, as they are collected by non-specialists using non-reference methods. The quality of the citizen-collected data might vary depending on the design of the CS project. For instance, projects that engage volunteers to collect data regardless of the quality of the outcomes are prone to high error rates associated with citizens' measurements. On the other hand, projects that include a training phase as well as precise monitoring guidelines before the start of the data collection should expect less errors, which helps the validation process of the data. Yet, there is always a need for methods that aim at improving the final quality of CS-collected data if the goal is to combine them at some point with existing databases. Among these methods, data fusion techniques are widely found in the literature. They are based on the idea that combining at best information coming from different sources with unusual formats, different resolutions, units, and locations contributes to improve their final accuracy (see, e.g., Fasbender et al., 2009; Bogaert and Fasbender, 2007).

In order to improve water monitoring networks in Tunisia and since no existing CS initiatives were already reported to monitor water-related data in the country, the Together4Water project was started in October 2018 in collaboration with local Tunisian institutes and schools (see Together4Water homepage) in a test region "Medjez-El-Beb city" (Fehri et al., 2020). The project aims at engaging the population in environmental monitoring and knowledge generation to support the existing water-related databases. This should also foster the local communities' awareness about their environment and empower them to take actions and contribute to the sustainable management of water resources. Consequently, one goal of the project is to involve citizens from different generations in monitoring discharge of the Medjerda river at two different locations (denoted Medjez-N5 and Slouguia) using the publicly available smartphone application "Discharge app" that estimates river discharge based on the processing of a five-seconds video recording (Photrack, 2018a). The application was first successfully used by the "Global iMoMo Initiative" to monitor discharge of the Themi River in Tanzania in collaboration with local stakeholders (Photrack, 2018b). In our study case, more attention will be paid to the validation of the citizen-based data as well as to the fusion of the various measurements.

In the first part of this paper, we will shortly describe the CS approach that is adopted to engage citizens in the region and the way they were trained to properly use the smartphone application. We subsequently assess the quality of the CS-based discharge measurements by comparing them to two official reference stations located at the same places and maintained by the local water authority. In the second part of the paper, a fusion of these citizens-based measurements is proposed using a Best Linear Unbiased Predictor (BLUP) approach, that aims at combining them for obtaining a single and improved estimation. Results of this data fusion will be compared to the reference discharges in order to assess the quality of the prediction. Two main objectives will thus be achieved here, i.e. (i) to show that citizens-based discharge measurement using a smartphone application can provide sound estimation of the real discharge and (ii) to emphasize that data fusion is relevant for combining these measurements, thus delivering higher quality data at the end. As this quality is depending both on the measurement errors caused by the citizens and by the smartphone application, a special attention will be paid to the assessment of the respective contribution of these two sources of errors.

2. Materials and methods

2.1. Study area

Known for its strategic location in North Tunisia, the test region "Medjez-El-Beb city" is located in the center of the Medjerda basin (see Fig. 1), about 60 km from Tunis (the capital of Tunisia) and 50 km from Beja (the capital of the governorate). The study area is characterized by a semi-arid climate with an average annual rainfall of 420 mm (DGRE, 2016). The Medjerda catchment is the most important freshwater resource in the country. It covers a total area of 23,700 km^2 of which 33% are located in Algeria. About 84% of the basin water resources are used for agricultural purposes, while about 10% are used for services and industries (Fehri et al., 2019). Similarly, the main economic activities of the Medjez-El-Beb region are related to agriculture and agri-food industries that exert significant pressure on the available water resources. The population within the city of Medjez-El-Beb has been growing significantly over the last two decades, from 38,964 in 2004 to 41,749 in 2014 (INS, 2014). Multiple schools, institutes and NGO's are located in the city, which represents a suitable environment for citizen science activities.

The city of Medjez El Beb provides easy access to the existing discharge monitoring sites. The official discharge monitoring in the study area consists of two hydrometric stations (namely Medjez-N5 and Slouguia). The monitoring method includes automated stations based on water level radar sensors for measuring open channel flow. These stations send daily measurements to a centralized database. The hydrological regime at both sites is similar. The mean annual discharge is around 15 m^3/s and 17 m^3/s for Medjez-N5 and Slouguia, respectively,

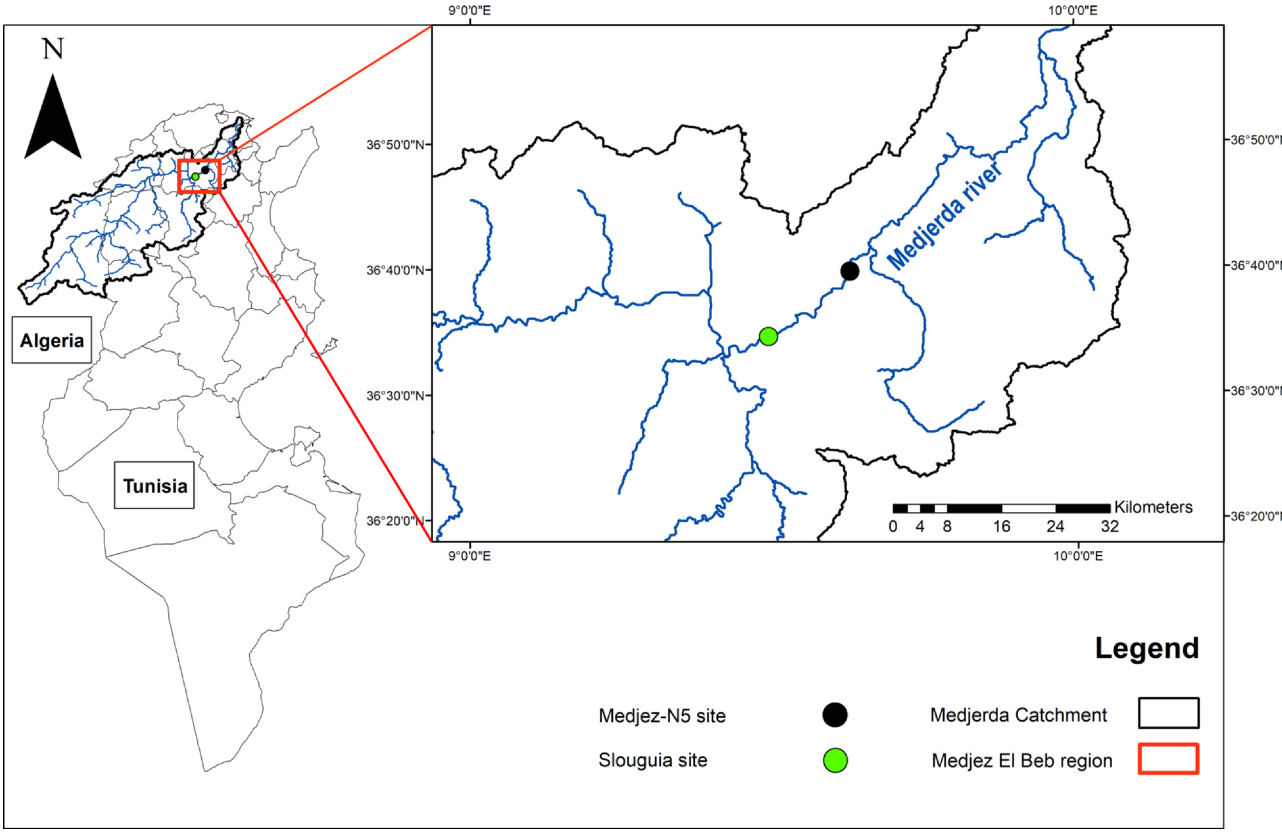

Fig. 1. Location of Medjez-N5 and Slouguia study sites.

while water level is typically ranging from 0.7 to 1.8 m for Medjez-N5 and from 0.8 to 2 m for Slouguia. The physical characteristics of both sites are quite similar too, with cross-section lengths of 29 m and 30 m at Medjez-N5 and Slouguia, respectively.

2.2. Citizens engagement methodology

Thanks to its high demography and diversified activities in both rural and non-rural environments, the Medjez-El-Beb city fulfills appropriate conditions for a successful CS program. In the framework of the Together4Water project, the citizens involvement has been realised using a step-by-step CS approach (Fehri et al., 2020) in order to ensure consistent and reliable discharge data collection using the publicly available smartphone application “Discharge app”. Citizens were first reached in the region via the project website, that includes a detailed presentation of the project’s goals and the available monitoring tools. The website was advertised on the local social media and at the schools and universities of the region, with the aim of reaching a wide and diversified panel of people. A total of 20 candidate citizens from different educational backgrounds and generations were afterwards selected to perform the discharge measurements based on their motivation, their location (close to the measurement sites), the fact that they own a smartphone, and their access to an internet connection. The final step of the engagement process consisted in providing them a complete field training for proper use of the measurement tool as well as for proper data transmission. The training program was organized in the framework of group meetings with citizens at the monitoring sites. Assistance was provided to explain the different steps of the measurement such as locating the sites created on the app, choosing the right standing position located on one of the riverbanks, and filming a 5-s video with steady hands to avoid low quality videos. A specific attention was paid to the data transmission process, which can be made immediately after the processing of the video. In addition, a list of factors that can affect the quality of the measurement was delivered and explained to citizens such as the presence of wind, light reflection on the water surface, and the color of the water. The knowledge of the impact of these factors is crucial to help citizens evaluate the quality of the measurements on site and to make multiple measurements if needed. The entire training program was video-recorded and documented in a public handbook distributed to citizens. This preparation and training step was crucial in order to ensure consistent data collection and to reduce knowledge-related issues at the start of the measurement campaign. In this study, we present the outcomes of eight citizens (four citizens per measuring site) who collected the most data from the start of the monitoring campaign.

2.3. Mobile phone discharge application

In this study, a publicly available smartphone application named “Discharge app” was used. The application was developed by Photrack (2018a) as a cost-effective measurement tool. The Discharge app (available for Android devices) uses the smartphone’s built-in camera and accelerometer to optically measure open channels’ water level and surface velocity and therefore to derive an estimation of the discharge (Carrel et al., 2019; Lüthi et al., 2014). The approach is based on the Surface Structure Imaging Velocimetry (SSIV) technique, which is a correlation-based technique typically applied to large channels or rivers, similar to Large Scale Particle Imaging Velocimetry (LSPIV) approach (Kantoush et al., 2011; Fujita et al., 1998).

For a proper use of the mobile phone app, a technical field preparation and setup was first needed, as described in the Discharge app developers’ instructions guide (Carrel et al., 2019). Four markers were positioned on both riverbanks (Fig. 2 and a geometrical survey was performed at both sites in order to gather information about the exact position of the markers, the cross-section of the river, and the shoreline. For this last task, a Disto S910 telemeter (*Leica*^{TM}) was used. The cross-

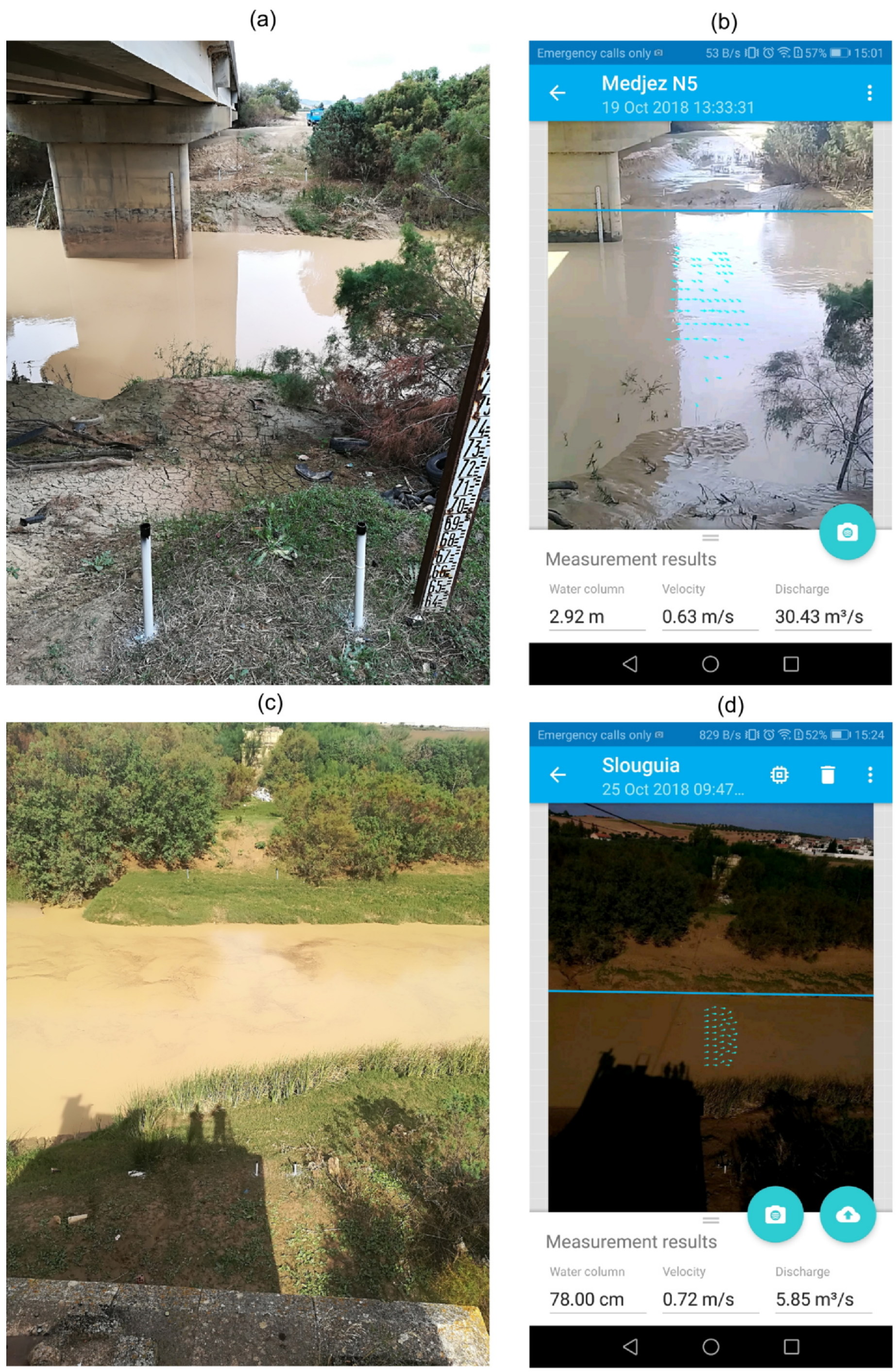

Fig. 2. Picture of the reference sites with corresponding screenshots of the smartphone application for two events. Parts (a) and (b) refer to the Medjez-N5 site, while Parts (c) and (d) refer to the Slouguia site.

sections obtained at both sites were encoded into the Discharge app, along with the Manning–Strickler coefficient. The video resolution of the mobile phone was set at its highest value in order to maximize the accuracy of the results. As an illustration, Fig. 3 presents a screenshot of the application with the window where this information was encoded. The main steps of Discharge estimation can be described as follows: (i) the selection of the implemented site (Fig. 3); (ii) a five-seconds video of the river flow is to be recorded. Instructions for the recording are user-specific and related to the user's standing position and the selection of the water column; (iii) after locating the four markers on both riverbanks, the intersection between the water surface and the shoreline is manually defined to characterize the actual water level (the blue line in Fig. 2b and d); (iv) finally, the recorded video is processed locally on the smartphone using the SSIV algorithm. The estimated discharge as well as the surface velocity are then displayed (Fig. 2). The theoretical aspects of the Discharge app are detailed and described by Carrel et al. (2019), Lüthi et al. (2014) and Leitão et al. (2018).

Using this mobile phone app, the data collection campaign started in October 2018 at both sites, where citizens were in charge of measuring the river discharge for a same series of hydrological events. Measurements were uploaded via the app itself to a cloud-based online platform where all measurements can be accessed for all citizens in a structured database, including the date and hour of the measurement along with the name of the volunteer. A total of 100 events were

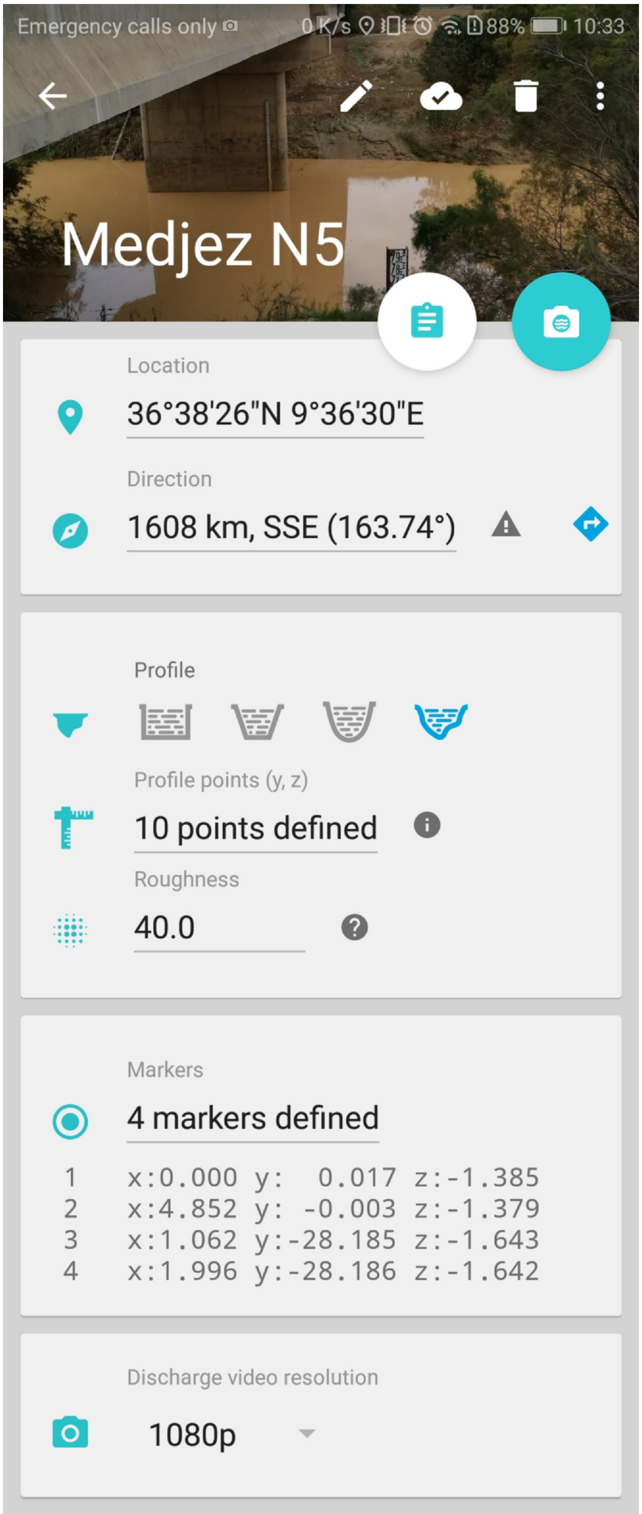

Fig. 3. Screenshot of the mobile phone app with the encoded parameters at the Medjez-N5 site.

monitored by eight citizens (four citizens per site), but only a part of them was considered in this study, covering the period from October 2018 to October 2019.

2.4. Data fusion and prediction of discharge

Let us consider a given hydrological event for which the true discharge is denoted by z, while the various discharge measurements as collected from n distinct users at the same location are given by $Y_1, \ldots, Y_n$. Let us consider that we can assume that $E[Y_i|z] = z$, i.e. on the average these users measurements correspond to the true discharge z. Stated in other words, the regression $E[Y|z]$ is the 1:1 line and users are all providing distinct but unbiased measurements of the true discharge z. Generalizing this for any event such that Z is a random variable too, we can thus consider the random model

$$Y_i = Z + \varepsilon_i \quad \forall\, i = 1, \ldots, n \quad \Leftrightarrow \quad \mathbf{Y} = Z\mathbf{1} + \boldsymbol{\varepsilon} \tag{1}$$

(with $\mathbf{1}$ the unit column vector of size n) where Z is the single true but unknown discharge and where $\mathbf{Y} = (Y_1, \ldots, Y_n)'$ are the various corresponding users measurements. From the fact that $E[Y_i|z] = z$, the errors $\boldsymbol{\varepsilon} = (\varepsilon_1, \ldots, \varepsilon_n)'$ are such that $E[\boldsymbol{\varepsilon}] = \mathbf{0}$ (with $\mathbf{0}$ the null column vector of size n), with a covariance matrix Σ_ε. We will additionally consider that $Z \perp \boldsymbol{\varepsilon}$, i.e. the measurement errors $\boldsymbol{\varepsilon}$ are uncorrelated with the discharge Z.

In a data fusion framework, let us consider that what is sought for is a way to combine the various Y_i's in order to obtain a single predictor Z^p of the unknown discharge Z. One can rely on the Best Linear Unbiased Predictor (BLUP) of Z, i.e. the best linear combination $Z^p = \sum_i \lambda_i Y_i = \boldsymbol{\lambda}'\mathbf{Y}$ such that the prediction variance $Var[Z - \boldsymbol{\lambda}'\mathbf{Y}]$ is minimum subject to the unbiasedness constraint $E[Z - \boldsymbol{\lambda}'\mathbf{Y}] = 0$, where $\boldsymbol{\lambda} = (\lambda_1, \ldots, \lambda_n)'$ is a vector of weights that need to be estimated. This can be done using the Lagrangian formalism, where the objective function

$$L(\boldsymbol{\lambda}, \eta) = Var[Z - \boldsymbol{\lambda}'\mathbf{Y}] + 2\eta E[Z - \boldsymbol{\lambda}'\mathbf{Y}] \tag{2}$$

needs to be minimized with respect to the weights $\boldsymbol{\lambda}$ and to the Lagrangian multiplier η. Eq. (2) can however be strongly simplified. Using Eq. (1), the unbiasedness constraint can be rewritten as

$$\begin{aligned} E[Z - \boldsymbol{\lambda}'\mathbf{Y}] &= E[Z] - E[Z]\boldsymbol{\lambda}'\mathbf{1} - \boldsymbol{\lambda}'\overbrace{E[\boldsymbol{\varepsilon}]}^{=0} \\ &= E[Z](1 - \boldsymbol{\lambda}'\mathbf{1}) = 0 \end{aligned}$$

so that the unbiasedness condition to be fulfilled is $\boldsymbol{\lambda}'\mathbf{1} = 1$, i.e. the weights must sum up to one. Using again Eq. (1), the predictor variance can now be rewritten as

$$\begin{aligned} Var[Z - \boldsymbol{\lambda}'\mathbf{Y}] &= Var\left[Z\overbrace{(1 - \boldsymbol{\lambda}'\mathbf{1})}^{=0} - \boldsymbol{\lambda}'\boldsymbol{\varepsilon}\right] \\ &= Var[\boldsymbol{\lambda}'\boldsymbol{\varepsilon}] = \boldsymbol{\lambda}'\Sigma_\varepsilon\boldsymbol{\lambda} \end{aligned} \tag{3}$$

Plugging these two results in Eq. (2) now gives the classical problem of minimizing

$$L(\boldsymbol{\lambda}, \eta) = \boldsymbol{\lambda}'\Sigma_\varepsilon\boldsymbol{\lambda} + 2\eta(1 - \boldsymbol{\lambda}'\mathbf{1})$$

where $\boldsymbol{\lambda}'\Sigma_\varepsilon\boldsymbol{\lambda}$ is a quadratic form, so that the minimum is unique and is reached when

$$\begin{cases} \frac{\partial L(\boldsymbol{\lambda},\eta)}{\partial \boldsymbol{\lambda}} = \mathbf{0} \\ \frac{\partial L(\boldsymbol{\lambda},\eta)}{\partial \eta} = 0 \end{cases} \Leftrightarrow \begin{cases} 2\Sigma_\varepsilon\boldsymbol{\lambda} + 2\eta\mathbf{1} = \mathbf{0} \\ 1 - \boldsymbol{\lambda}'\mathbf{1} = 0 \end{cases} \Leftrightarrow \begin{pmatrix} \Sigma_\varepsilon & \mathbf{1} \\ \mathbf{1}' & 0 \end{pmatrix}\begin{pmatrix} \boldsymbol{\lambda} \\ \eta \end{pmatrix} = \begin{pmatrix} \mathbf{0} \\ 1 \end{pmatrix}$$

Solving this linear system of equations leads to the solution

$$\boldsymbol{\lambda} = \frac{1}{\mathbf{1}'\Sigma_\varepsilon^{-1}\mathbf{1}}\Sigma_\varepsilon^{-1}\mathbf{1} \tag{4}$$

(where $\mathbf{1}'\Sigma_\varepsilon^{-1}\mathbf{1}$ is a scalar), with an associated prediction variance as given by Eq. (3) and thus equal to

$$Var\left[Z - \boldsymbol{\lambda}'\mathbf{Y}\right] = \frac{1}{\mathbf{1}'\Sigma_\varepsilon^{-1}\mathbf{1}} \tag{5}$$

Eqs. (4) and (5) thus provide a way to fuse the various discharge measurements $\mathbf{Y}$ in order to predict at best the unknown discharge Z, by providing a set of weights $\boldsymbol{\lambda}$ and an associated prediction variance $Var[Z - \boldsymbol{\lambda}'\mathbf{Y}]$ which is measuring the performance of this predictor Z^p.

2.5. Sources of errors

In the previous section, we focused on the BLUP without any specific hypothesis on the covariance matrix Σ_ε, so that these results hold true in general. We will now focus on the structure of Σ_ε by considering mixed sources of errors of various origins. The first possible origin is a random error ε_m linked to the event, that is assumed to be random (i.e., this error will vary from one event to another one) but that affects identically all users for the same event. For our case study, this error could be linked to the smartphone application that underestimate or overestimate in a similar way for all users the discharge value of a given event, while this error differs between events. A second possible origin is a random error $\varepsilon_{u,i}$ linked to the user itself, that can be assumed as independent between users and independent from ε_m, with a variance that only depends on the user.

These sources of errors (the smartphone application and the users) were considered based on the fact that they can easily be interpreted, which led to this simple and classical decomposition of errors. On the other hand, a possible site effect could also be considered, but due to the fact that only two sites were at hand, no clear conclusions could be drawn, and it would be impossible to reliably estimate this kind of effect in the context of a random factors model. Furthermore, it is quite possible (and even likely) that pure random errors exist, but they could not be assessed from the data at hand. Indeed, this would require repeated measurements for the same citizen and the same event. If such pure random errors exist in our data, they are thus included into the user's variance in our model. It is worth mentioning that crossed effect between the user and the event might be possible and is not theoretically impossible, although, it would be unlikely at the same time, at least if the measurement conditions of the same event are comparable for all users. In such conditions, it is hard to imagine how there could be an interaction between the event and the user. Nevertheless, it remains true that our model could possibly include pure random errors and/or interaction effects, as long as these effects can be assessed from the data at hand and that there is some evidence to consider them in the model. It is unfortunately not the case for our data.

Stated in other words, considering that $E[\varepsilon_m]=0$ and $E[\varepsilon_{u,i}]=0$ and assuming first that all users have a similar variance of errors, we now have

$$\boldsymbol{\varepsilon} = \varepsilon_m \mathbf{1} + \boldsymbol{\varepsilon}_u$$

where ε_m is a scalar and $\boldsymbol{\varepsilon}_u = (\varepsilon_{u,i}, \ldots, \varepsilon_{u,n})'$, so that

$$\Sigma_\varepsilon = \sigma_m^2 \mathbf{1}\mathbf{1}' + \sigma_u^2 \mathbf{I} \tag{6}$$

(with $\mathbf{I}$ the identity matrix), where σ_m^2 and σ_u^2 are the measuring device's and user's variance, respectively. The corresponding correlation matrix is given by

$$\mathbf{R}_\varepsilon = \mathbf{D}_\varepsilon^{-1/2} \Sigma_\varepsilon \mathbf{D}_\varepsilon^{-1/2}$$

where $\mathbf{D}_\varepsilon = diag(\Sigma_\varepsilon)$. Using Eq. (6), this gives $\mathbf{D}_\varepsilon = (\sigma_m^2 + \sigma_u^2)\mathbf{I}$ and so the (i, j) element of $\mathbf{R}_\varepsilon$ is then given by

$$r_{ij,\varepsilon} = \frac{\sigma_m^2}{\sigma_m^2 + \sigma_u^2} \quad \forall\ i \neq j \tag{7}$$

where $r_{ij,\varepsilon}$ (also known as the intraclass correlation coefficient in the random model terminology) is the correlation between the measurements of the ith and jth users when they are measuring the discharge for the same event. As seen from Eq. (7) and under the condition of Eq. (6), this correlation coefficient corresponds to the part of the variance that comes from the measuring device, where $\sigma_m^2 + \sigma_u^2$ is the total variance. Under the condition of Eq. (6) again, it can also be proved that all weights must then be equal to $1/n$, so that $\boldsymbol{\lambda} = (1/n)\mathbf{1}$, and an explicit formulation for the prediction variance $Var[Z - \boldsymbol{\lambda}'\mathbf{Y}]$ as a function of n, σ_m^2 and σ_u^2 can also be obtained (see Appendix). In general, depending on training and experience, it could however be expected that the same variance σ_u^2 does not necessarily hold for all users, so that Eq. (6) is more generally written as

$$\Sigma_\varepsilon = \sigma_m^2 \mathbf{1}\mathbf{1}' + \mathbf{D}_u \tag{8}$$

where $\mathbf{D}_u$ is a diagonal matrix having $\sigma_{u,i}^2$ as ith element (i.e., the variance for the ith user) and where the weights $\boldsymbol{\lambda}$ are then no more identical in that case.

As the predictor $Z^p = \boldsymbol{\lambda}'\mathbf{Y}$ is a linear combination of users measurements $\mathbf{Y}$, the prediction error $Z - \boldsymbol{\lambda}'\mathbf{Y}$ will tend to be Gaussian distributed as long as the correlation between these measurements (as measured by Eq. (7)) is not too high. It is then possible to provide a simple prediction interval to the discharge Z. Assuming that

$$Z - \boldsymbol{\lambda}'\mathbf{Y} \sim N(\mu_p, \sigma_p^2)$$

with $\mu_p = E[Z - \boldsymbol{\lambda}'\mathbf{Y}] = 0$ from the unbiasedness condition and with $\sigma_p^2 = Var[Z - \boldsymbol{\lambda}'\mathbf{Y}]$ as computed from Eq. (5), two-sided prediction interval at the $1-\alpha$ confidence level is then

$$-z_{1-\alpha/2} \leqslant \frac{Z - \boldsymbol{\lambda}'\mathbf{Y}}{\sqrt{\sigma_p^2}} \leqslant z_{1-\alpha/2}$$

or equivalently

$$\boldsymbol{\lambda}'\mathbf{Y} - z_{1-\alpha/2}\sqrt{\sigma_p^2} \leqslant Z \leqslant \boldsymbol{\lambda}'\mathbf{Y} + z_{1-\alpha/2}\sqrt{\sigma_p^2} \tag{9}$$

where $z_{1-\alpha/2}$ is the $1-\alpha/2$ quantile of the zero-mean unit variance Gaussian distribution. This confidence interval will narrow when n is increased, but it is incorrect to state that $lim_{n\to\infty}\sigma_p^2 = 0$ in general, except when $\sigma_m^2 = 0$. Stated in other words, increasing the number n of users measurements will help to reduce the uncertainty about Z, but there is a lower bound equal to σ_m^2 for the prediction variance, that relates to the errors ε_m which cannot be reduced by increasing n. The proper estimation of σ_m^2 and σ_u^2 is thus important, as these variances are conditioning the sampling strategy, i.e. by assessing the benefit of including more users in the process or the benefit of improving the measuring device for reducing σ_m^2. In practice, the estimation of σ_m^2 and σ_u^2 can be done from a set of observed hydrological events and user measurements using any standard statistical computer package. Indeed, Eq. (1) corresponds to a one-way ANOVA model with random effect, so that a Restricted Maximum Likelihood (REML) procedure can be used for estimating at best these variance components. See, e.g., Galecki and Burzykowski (2013) and Fox (2008) for a presentation of the details related to random models and the corresponding estimation procedures.

3. Results and discussion

A careful quality assessment of the CS-based discharge measurements is crucial, both for evaluating the performance of the smartphone application and for assessing the consistency of these measurements over time. With these goals in mind, extreme discharge events (that represent four events out of the total) were excluded from our analysis at both sites, since measurements were inaccurate due to the difficulty of locating the markers on both sides of the river, as caused by the high water level during these events. Therefore, only discharge measurements corresponding to values lower than 35 m^3/s were considered in this analysis. This represents 90% of the collected data. More precisely, 90 events were considered in this study, where each event was monitored by the same four citizens at each study site.

3.1. Data quality assessment

Fig. 4 compares at the Medjez-N5 site the discharge measurements obtained from the reference station to those obtained from the four citizens using the application. In order to check for the possible presence of bias during the measurements, a regression line $E[Y_i|z] = \beta_{0,i} + \beta_{1,i}z$ was fitted for all citizens, leading to slope

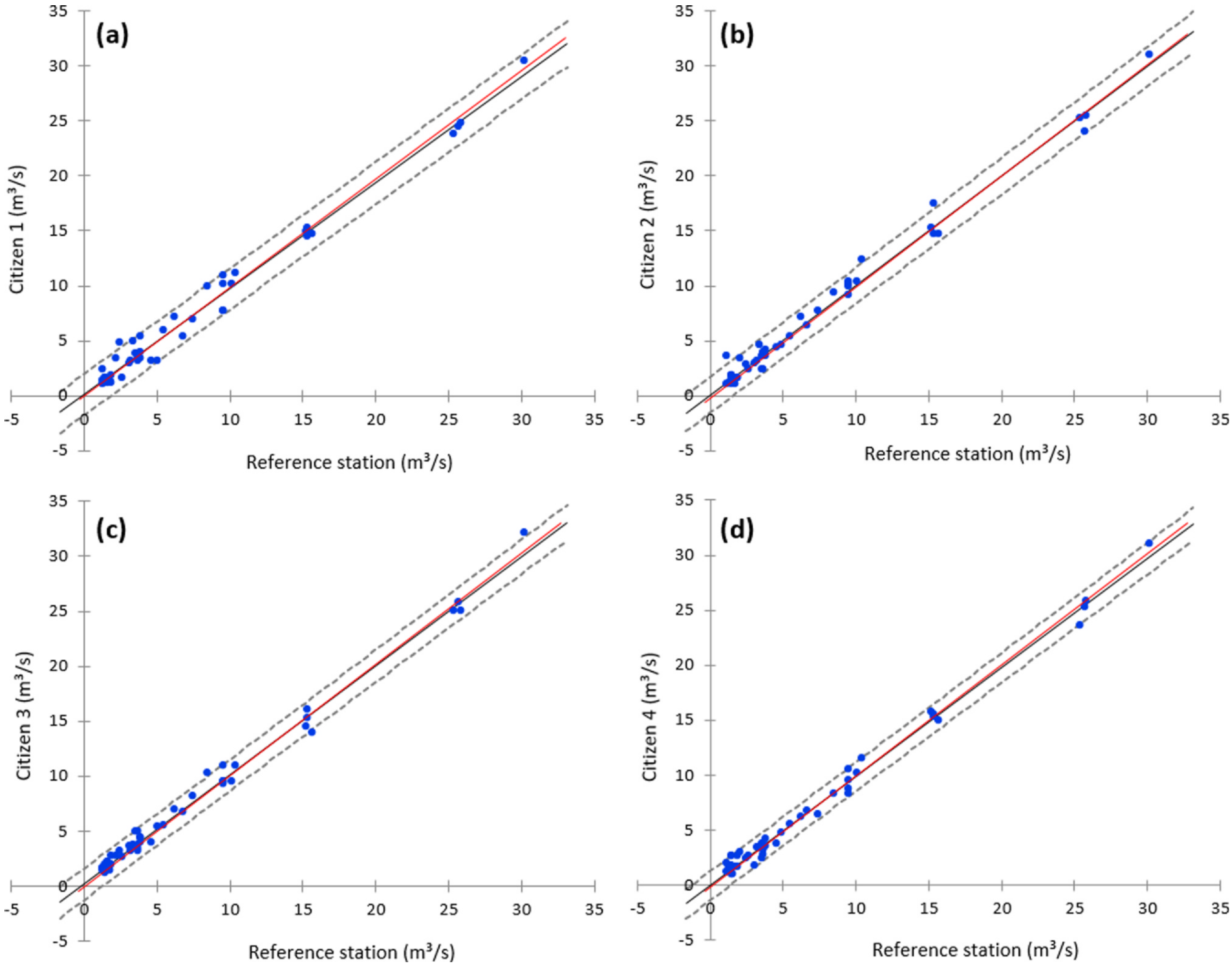

Fig. 4. Citizen-based versus reference-based discharge measurements at the Medjez-N5 site, along with the 1:1 line (black plain line), the estimated regression line (red plain line), and the corresponding 95% prediction interval (dashed lines). (For interpretation of the references to color in this figure legend, the reader is referred to the web version of this article.)

estimates $\widehat{\beta}_{1,i}$ that range from 0.992 to 0.996. However, separate *F*-test based on the null hypothesis H_0: $\beta_{0,i} = 0,\ \ \beta_{1,i} = 1$ lead to the conclusion that these regression lines do not significantly differ from the 1:1 line ($p_v > 0.05$ for all citizens) and therefore citizens-based discharge measurements can be considered as statistically unbiased estimates of the true discharge (as evaluated from the reference station).

Although, small biases are always possible, but it appears to us that they could be neglected in our study. For practical applications, it seems to us that what is relevant here is the effect of possible biases by comparison with other random effects. For our data, it is clear that biases can be neglected, as long as we refer to the official gauging stations as our reference data. If the conclusion of the test would have been that biases exist, they must ideally be accounted for in the model, as long as their impact is not minimal for the final results. If these biases are coming from the users, this would lead to considering that measurements from each user should be corrected for each user's bias prior to the data fusion. If these biases come from systematic errors, they would be however much more complicated to assess, as doing so would require other reference data (ideally the real discharge values) for comparison purposes. It is still possible to conduct a sensitivity analysis in order to assess the impact that a misspecification (e.g., in the conversion of surface velocities to depth-average velocities) might have, but still this would not allow us to assess the real impact of these misspecifications without additional reference data or alternate measurement methodologies, again for comparison purposes.

Besides the absence of bias, the R^2 values are ranging from 0.984 to 0.990 and thus indicate a good agreement between citizen-based and reference-based measurements. Similar observations and conclusions can be made for all citizens at the Slouguia site (not shown here). One can also see that the pattern of deviations from the 1:1 line is comparable between citizens, thus suggesting that the training provided at the start of the campaign was beneficial, as these citizens were from different generations and educational backgrounds.

3.2. Distribution of the errors

Focusing on the measurements errors for each citizen, it is possible to test the equality of variance between citizens, as well as to test the hypothesis that these errors are Gaussian distributed for each citizen. It's worth noting that the official discharge measurements are prone to errors. However, the data provider does not communicate the information about these errors. Accordingly, the additional variance that might be induced by such errors is not accounted for here. Variance equality was tested using the Levene's test (Levene, 1960; Iachine et al., 2010), that leads to the conclusion they can be assumed as equal between citizens for both sites (with $p_v = 0.157$ and 0.319 at the Medjez-N5 and Slouguia sites, respectively). Normality was tested separately for each citizen using the Shapiro–Wilk test (Shapiro and Wilk, 1965) and leads to the conclusion that measurement errors can be assumed as normally distributed for all citizens at both sites too (with $p_v > 0.05$ for

Table 1
Sample statistics and p-values (p_v) of the Shapiro–Wilk's test for citizens-based (C_i) discharges at both sites, where left and right parts of the table refer to the Medjez-N5 and Slouguia site, respectively. Values $y_{(1)}$, $y_{(n)}$, $\bar{y}$ and σ are the minimum, maximum, mean and standard deviation, respectively.

	C_1	C_2	C_3	C_4	C_1	C_2	C_3	C_4
$y_{(1)}$	−1.908	−1.580	−1.800	−1.770	−1.097	−1.699	−1.699	−1.398
$y_{(n)}$	2.239	2.330	1.930	1.190	1.303	1.919	1.944	1.908
$\bar{y}$	−0.163	0.063	0.144	−0.102	−0.083	−0.184	−0.086	−0.178
σ	0.945	0.793	0.695	0.640	0.670	0.854	0.847	0.697
W	0.970	0.941	0.963	0.974	0.922	0.985	0.952	0.957
p_v	0.273	0.219	0.141	0.371	0.145	0.959	0.245	0.308

all citizens; see Table 1).

Errors can be expected as being proportional to discharge in general, and this was partly observed on the raw data, that included 10% of discharge values that were above 35 m^3/s. From the examination of measurements above that threshold (not shown in the paper), they were considered as quite unreliable and they are also associated with extreme events, for which the measurement app is not expected to deliver sound results. These values were thus discarded. For the 90% of values below that threshold, no proportional effect can be observed, as illustrated in Fig. 4. Hence, the assumption of a constant variance of errors for citizen-based discharge below the 35 m^3/s threshold seems valid. Although Fig. 4 might show slightly wider and narrower uncertainty interval between users (especially for citizen 1 and 3), the Levene statistical test confirms that all variances can indeed be considered as identical. Though the bivariate scatterplots might appear as different, testing the equality of variance only relies on the data used to build the histograms that appear on the diagonal in Fig. 5 (that are not so different). It is worth noting too that the number of measurements is limited, so (i) the statistical power of the Levene test (i.e. its ability to detect a difference between variances when it exists) is not very high, and (ii) few values might appear as more isolated on the histograms, thus giving the impression that the distributions are different as well.

3.3. Variance decomposition

In order to assess the amount of intraclass correlation as defined by Eq. (7), one can estimate the Pearson correlation coefficient $\hat{r}_{ij}$ between CS-based discharge that are measured for the same set of events, as presented in Fig. 5 for the Medjez-N5 site. All correlations are statistically significant (p_v > 0.05) and range from 0.33 to 0.48, except between citizens 3 and 4 at the Medjez-N5 site. Comparable results (not shown here) are obtained at the Slouguia site.

The fact that these correlations are significant and comparable between citizens is in agreement with the hypothesis that the total

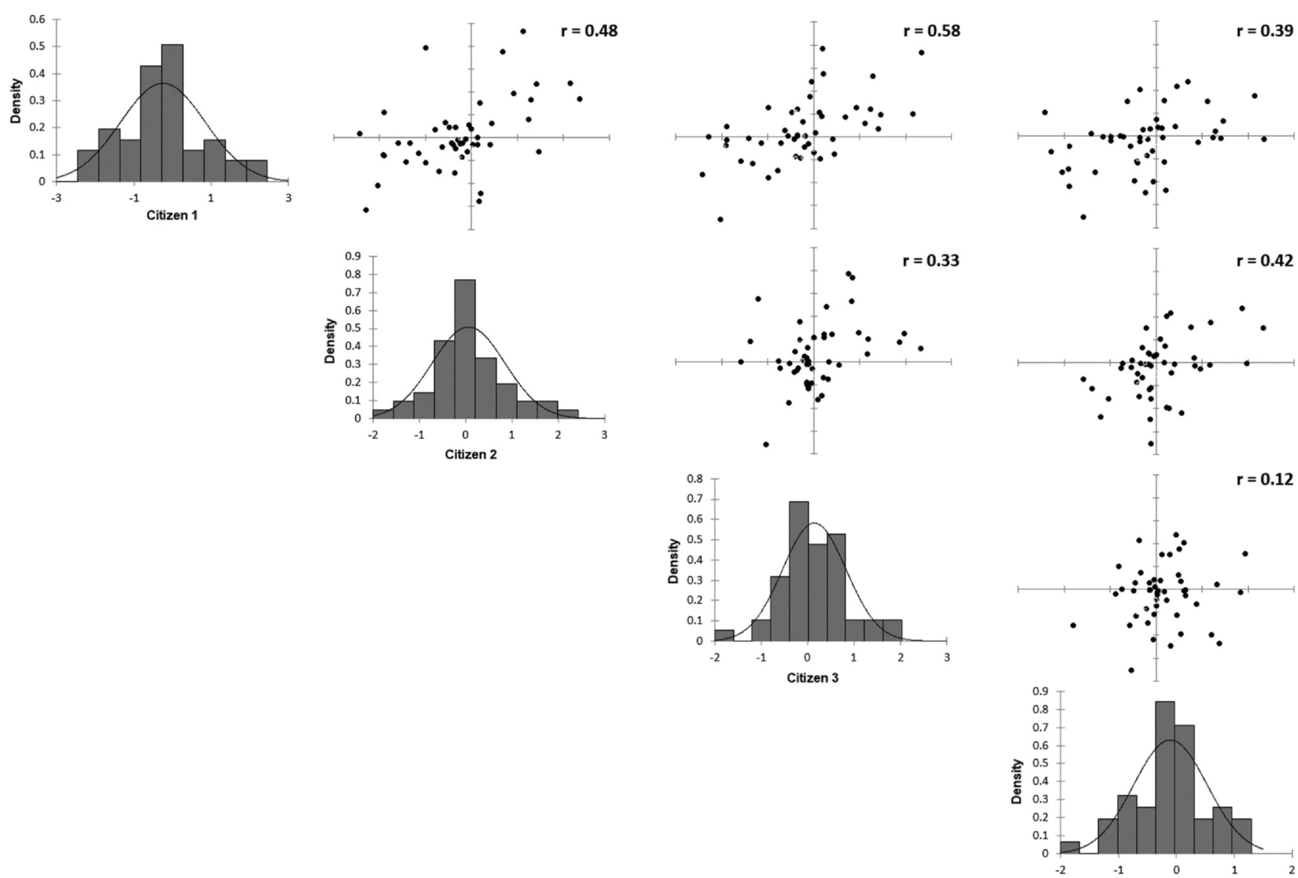

Fig. 5. Histograms (on diagonal) and scatterplots (off diagonal) of the discharge residuals for the 4 citizens at the Medjez-N5 site, with corresponding correlation coefficients between citizens' discharge measurements for the same events.

Table 2
REML estimates of σ_m^2 and σ_u^2 at the Medjez-N5 and Slouguia sites, along with their respective contribution (in %) to the total variance $\sigma_m^2 + \sigma_u^2$.

	Medjez-N5	Slouguia
σ_m^2	0.259 (36.8%)	0.398 (38.7%)
σ_u^2	0.444 (63.2%)	0.630 (61.3%)
total	0.703 (100%)	1.028 (100%)

variance of errors can indeed be decomposed in two parts, as suggested in Section 2.5, where σ_m^2 is the part of the variance linked to the smartphone application while $\sigma_{u,i}^2$ is the part linked to each citizen. As the hypothesis of variance equality between citizens has already been accepted in Section 3.2, we can consider that $\sigma_{u,i}^2 = \sigma_u^2$ for all citizens, so that a single σ_u^2 value need to be estimated for each site.

Being able to assess the respective amount of each source of errors is important in our context, as it eases the identification of the part of the measurement chain that need to be improved in priority. It also allows us to assess the expected benefit of increasing the number of citizens measuring the same event in order to reduce the error, knowing that σ_m^2 is a lower bound for the total variance, as previously explained. Based on a one-way ANOVA model with random effect and using a REML procedure, the corresponding results are given in Table 2. It can be seen that the estimated part of the variance σ_m^2 related to the smartphone application is equal to 37% and 39% of the total variance at the Medjez-N5 and Slouguia sites, respectively, so that the variance σ_u^2 attributed to the citizens account for more than 60 % of the total at both sites.

As stated before, ε_m represents the random error related to the event, which varies between events but which identically affects all citizens for the same event. In our study, the main reason for this effect is attributed to the smartphone application. Its importance can be reduced by improving the sites setup by using a better geometrical survey of the cross-section, with more visible markers at both river banks (especially for high discharge events). In parallel, a better estimation of the Manning–Strickler coefficient that was empirically selected and encoded in the application, is expected to reduce this random error and lead to an improved discharge estimation. On the other hand, the $\varepsilon_{u,i}$ error is related to the user itself and depends on various factors such as the citizen's position on the riverbank while recording the video sequence, the absence of hand movement during the recording, and the quality of the camera of the citizen's mobile phone (mainly in terms of video resolution). With respect to the reference data, it is worth mentioning that the official measurements at both sites are also affected by errors. However, the quantitative information about these errors is not available and is limited to specific governmental institutions.

3.4. Data fusion

Following the reasoning in Sections 2.4 and 2.5, one can use Eqs. (4) and (5) for fusing the various CS-based discharge measurements of the same event and for providing a two-sided prediction interval for the true discharge using Eq. (9). Corresponding results are shown in Fig. 6 for both sites. For the sake of comparison with the initial results obtained separately for each citizen, Table 3 provides the estimated variances of the errors around the 1:1 line, along with the corresponding R^2 values.

One can see from the reduced S^2 and increased R^2 values that fusing CS-based discharge measurements leads to improved results, with a good agreement between the fused predicted discharges and the reference discharge at both sites. The 95% prediction intervals that are obtained under a Gaussian distribution hypothesis are thus reduced and remain in good agreement with the fused data as well. Though the benefit of the fusion procedure might appear as modest here, it should also be reminded that (i) σ_m^2 (the part of the variance that cannot be reduced by fusing measurements) represents here about 40% of the total variance at both sites, and (ii) the fusion only involved eight

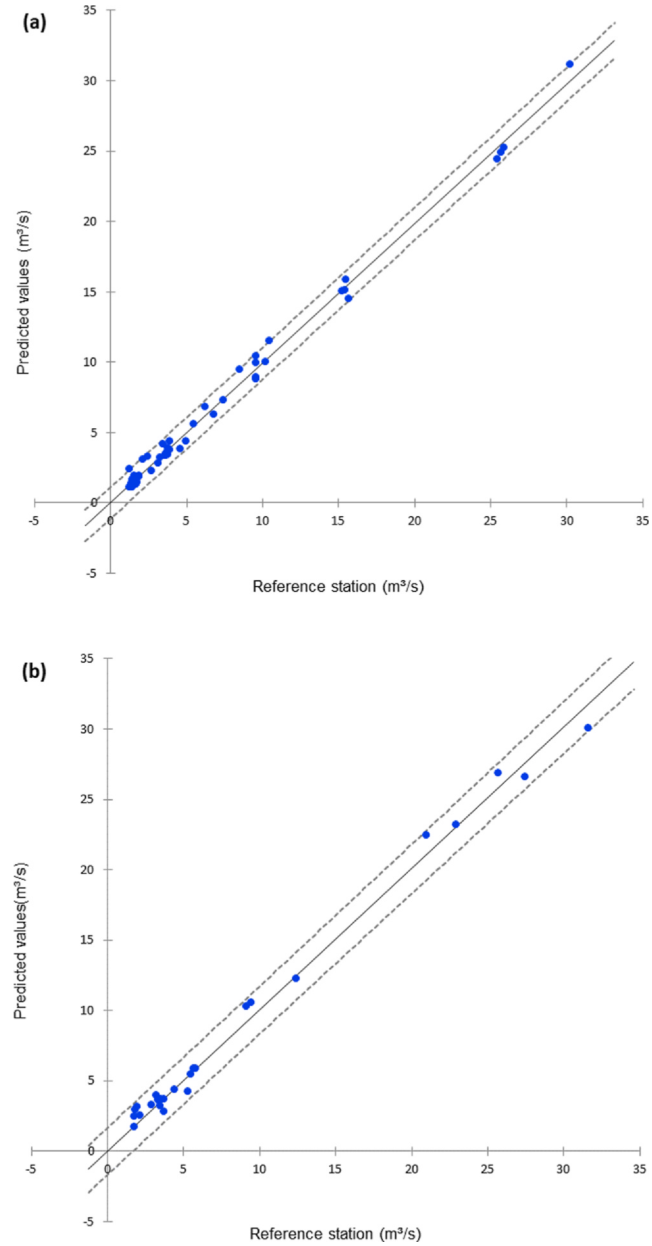

Fig. 6. Predicted (fused) citizens-based discharges versus reference discharges, along with the corresponding prediction intervals (dashed lines) around the 1:1 line (plain line). Part (a) refers to the Medjez-N5 site, while Part (b) refers to the Slouguia site.

Table 3
Estimated variances S_i^2 of the four citizens-based (C_i) discharge errors around the 1:1 line and the corresponding R_i^2 values, along with the results for the fused measurements (last line). Left and right parts of the table refer to the Medjez-N5 and Slouguia site, respectively.

C_i	S_i^2	R_i^2	S_i^2	R_i^2
1	0.8737	0.9838	1.1557	0.9854
2	0.6157	0.9883	2.1590	0.9720
3	0.4722	0.9897	1.2191	0.9859
4	0.4002	0.9894	0.9815	0.9875
fused	0.2682	0.9970	0.4141	0.9960

citizens' measurements in our study. As a result, the fusion procedure leads here to a moderate reduction of the total variance, but this variance reduction can however greatly vary in general, depending on the study site and the number of involved citizens.

4. Conclusions

In the framework of the Together4Water project, discharge data were collected for a series of 90 hydrological events by a group of 8 citizens (4 citizens per site) using a publicly available smartphone application. In this paper, a Best Linear Unbiased Predictor (BLUP) method was used as a data fusion procedure in order to combine various CS-based discharge measurements at two locations along the Medjerda river, our test river in Tunisia. The major conclusions are as follows:

(1) The step-by-step CS approach used in this study was successful, as we were able to engage and motivate a group of citizens from different generations and educational backgrounds. The training program was crucial to streamline the data collection process before the start of the monitoring campaign, which helped to guarantee a consistent measurement of the discharge as well as appropriate data transmission.
(2) For low to moderate discharge values ($<35\ m^3/s$), the use of the mobile phone application provides promising results at both sites and for all users. The good quality (absence of bias and high correlation with true discharges) of these results was confirmed from the various analyses. For extreme discharge events ($>35\ m^3/s$), citizens were however unable to provide reliable measurements (difficulty to access the sites, to locate the markers on both sides of the river, etc.) and more work still needs to be done for handling these situations.
(3) A random model and a REML procedure were successfully used to model and to estimate the respective contribution of two sources of errors. For our study sites, these results have shown that the errors linked to the event/measuring device (ε_m) and to the users (ε_u) represent about 40% and 60% of the total variance, respectively. Reducing ε_m would require improving the mobile phone application and measuring conditions (more precise geometrical survey, better positioning of the markers, better estimation of the Manning–Strickler coefficient). Reducing the final impact of ε_u was however successfully done by simply fusing the various citizens' discharge measurements.
(4) Although no firm conclusions can be obtained so far for other sites that might present other challenges for collecting and fusing CS-based discharge measurements, this study still shows that the use of a low-cost measuring device (the smartphone application) by non-specialist volunteers (our trained citizens) is able to provide reliable results for discharge measurements and is thus a very promising approach for improving water discharge monitoring in countries that have limited monitoring networks.

CRediT authorship contribution statement

Raed Fehri: Project administration, Conceptualization, Methodology, Software, Data curation, Investigation, Writing - original draft. **Patrick Bogaert:** Conceptualization, Methodology, Visualization, Writing - original draft. **Slaheddine Khlifi:** Writing - review & editing, Supervision. **Marnik Vanclooster:** Writing - review & editing, Supervision.

Declaration of Competing Interest

The authors declare that they have no known competing financial interests or personal relationships that could have appeared to influence the work reported in this paper.

Acknowledgments

We acknowledge the support of the Université catholique de Louvain (UCLouvain), the Wallonie Bruxelles International (WBI) program and the Islamic Development Bank (IDB) Excellence Merit Scholarship. We sincerely thank all citizens who volunteered in the Together4Water project for their whole-hearted enthusiasm and dedication.

Appendix A

If we assume that Σ_ε is given by Eq. (6), it is possible to provide an explicit expression for Σ_ε^{-1} based on Miller (1981). In general, if $\mathbf{A}$ is a positive definite matrix and $\mathbf{B}$ is a matrix of rank 1, then

$$(\mathbf{A}+\mathbf{B})^{-1}=\mathbf{A}^{-1}-\frac{1}{1+g}\mathbf{A}^{-1}\mathbf{B}\mathbf{A}^{-1} \tag{A.1}$$

where $g = trace(\mathbf{A}^{-1}\mathbf{B})$. By identifying $\mathbf{A}=\sigma_u^2\mathbf{I}$ and $\mathbf{B}=\sigma_m^2\mathbf{1}\mathbf{1}'$ so that $\Sigma_\varepsilon^{-1}=(\mathbf{A}+\mathbf{B})^{-1}$ and knowing that $\mathbf{A}^{-1}=(1/\sigma_u^2)\mathbf{I}$, this gives after elementary manipulations

$$g=\frac{\sigma_m^2}{\sigma_u^2}n;\quad \frac{1}{1+g}=\frac{\sigma_u^2}{\sigma_u^2+n\sigma_m^2};\quad \mathbf{A}^{-1}\mathbf{B}\mathbf{A}^{-1}=\frac{\sigma_m^2}{\sigma_u^4}\mathbf{1}\mathbf{1}' \tag{A.2}$$

and so we obtain

$$\Sigma_\varepsilon^{-1}=\frac{1}{\sigma_u^2}\left(\mathbf{I}-\frac{\sigma_m^2}{\sigma_u^2+n\sigma_m^2}\mathbf{1}\mathbf{1}'\right) \tag{A.3}$$

which does not require the computation of any inverse matrix. Plugging this result in Eq. (4) now gives

$$\lambda \propto \Sigma_\varepsilon^{-1}\mathbf{1}=\frac{1}{\sigma_u^2}\left(1-\frac{n\sigma_m^2}{\sigma_u^2+n\sigma_m^2}\right)\mathbf{1} \tag{A.4}$$

where all factors in front of $\mathbf{1}$ are scalars, thus showing that all weights are the same and must be equal to $1/n$, as these weights sum up to one. Plugging this result in Eq. (5) finally gives

$$Var\left[Z - \lambda'\mathbf{Y}\right] = \frac{1}{\frac{n}{\sigma_u^2}\left(1 - \frac{n\sigma_m^2}{\sigma_u^2 + n\sigma_m^2}\right)} \tag{A.5}$$

References

Bogaert, P., Fasbender, D., 2007. Bayesian data fusion in a spatial prediction context: a general formulation. Stochastic Environmental Research and Risk Assessment 21 (6), 695–709.

Brakenridge, G.R., Nghiem, S.V., Anderson, E., Mic, R., 2007. Orbital microwave measurement of river discharge and ice status. Water Resources Research 43 (4), W04405. https://doi.org/10.1029/2006WR005238.

Buytaert, W., Zulkafli, Z., Grainger, S., Acosta, L., Alemie, T.C., Bastiaensen, J., De Bièvre, B., Bhusal, J., Clark, J., Dewulf, A., Foggin, M., Hannah, D.M., Hergarten, C., Isaeva, A., Karpouzoglou, T., Pandeya, B., Paudel, D., Sharma, K., Steenhuis, T., Tilahun, S., Van Hecken, G., Zhumanova, M., 2014. Citizen science in hydrology and water resources: opportunities for knowledge generation, ecosystem service management, and sustainable development. Frontiers in Earth Science 2, 26. https://doi.org/10.3389/feart.2014.00026.

Carrel, M., Detret, M., Peña-Haro, S., Lüthi, B., 2019. Evaluation of the DischargeApp: a smartphone application for discharge measurements. In: HydroSenSoft, International Symposium and Exhibition on Hydro-Environment Sensors and Software, Madrid, Spain, pp. 8.

Davids, J., Rutten, M., Pandey, A., Devkota, N., van Oyen, W., Prajapati, R., van de Giesen, N., 2019. Citizen science flow – an assessment of simple streamflow measurement methods. Hydrology and Earth System Sciences 23 (2), 1045–1065. https://doi.org/10.5194/hess-23-1045-2019.

DGRE, 2016. Rapport hydrologique 2016. Technical Report, Ministry of Agriculture, Water Resources and Fisheries; Tunis.

Dickinson, J.L., Shirk, J., Bonter, D., Bonney, R., Crain, R.L., Martin, J., Phillips, T., Purcell, K., 2012. The current state of citizen science as a tool for ecological research and public engagement. Frontiers in Ecology and the Environment 10 (6), 291–297. https://doi.org/10.1890/110236.

Dramais, G., Coz, J.L., Camenen, B., Hauet, A., 2011. Advantages of a mobile lspiv method for measuring flood discharges and improving stage-discharge curves. Journal of Hydro-environment Research 5 (4), 301–312. https://doi.org/10.1016/j.jher.2010.12.005. (iMAGE VELOCIMETRY).

Fasbender, D., Brasseur, O., Bogaert, P., 2009. Bayesian data fusion for space-time prediction of air pollutants: The case of no2 in belgium. Atmospheric Environment 43 (30), 4632–4645. https://doi.org/10.1016/j.atmosenv.2009.05.036.

Fehri, R., Khlifi, S., Vanclooster, M., 2019. Disaggregating SDG-6 water stress indicator at different spatial and temporal scales in Tunisia. Science of The Total Environment 694, 133766. https://doi.org/10.1016/j.scitotenv.2019.133766.

Fehri, R., Khlifi, S., Vanclooster, M., 2020. Testing a citizen science water monitoring approach in Tunisia. Environmental Science and Policy 104, 67–72. https://doi.org/10.1016/j.envsci.2019.11.009.

Fox, J., 2008. Applied Regression Analysis and Generalized Linear Models, second ed. Sage Publications.

Fritz, S., See, L., Carlson, T., Haklay, M.M., Oliver, J.L., Fraisl, D., Mondardini, R., Brocklehurst, M., Shanley, L.A., Schade, S., Wehn, U., Abrate, T., Anstee, J., Arnold, S., Billot, M., Campbell, J., Espey, J., Gold, M., Hager, G., He, S., Hepburn, L., Hsu, A., Long, D., Masó, J., McCallum, I., Muniafu, M., Moorthy, I., Obersteiner, M., Parker, A.J., Weisspflug, M., West, S., 2019. Citizen science and the united nations sustainable development goals. Nature Sustainability 2 (11), 1063. https://doi.org/10.1038/s41893-019-0426-8.

Fujita, I., Kunita, Y., Tsubaki, R., 2013. Image analysis and reconstruction of the 2008 toga river flash flood in an urbanised area. Australasian Journal of Water Resources 16 (2), 151–162. https://doi.org/10.7158/13241583.2013.11465411.

Fujita, I., Muste, M., Kruger, A., 1998. Large-scale particle image velocimetry for flow analysis in hydraulic engineering applications. Journal of Hydraulic Research 36 (3), 397–414. https://doi.org/10.1080/00221689809498626.

Galecki, A., Burzykowski, T., 2013. Linear Mixed-Effects Models Using R. Springer.

Hannah, D.M., Demuth, S., van Lanen, H.A.J., Looser, U., Prudhomme, C., Rees, G., Stahl, K., Tallaksen, L.M., 2011. Large-scale river flow archives: importance, current status and future needs. Hydrological Processes 25 (7), 1191–1200. https://doi.org/10.1002/hyp.7794.

Iachine, I., Petersen, H.C., Kyvik, K.O., 2010. Robust tests for the equality of variances for clustered data. Journal of Statistical Computation and Simulation 80 (4), 365–377. https://doi.org/10.1080/00949650802641841.

INS, 2014. Institut National de la Statistique, Tunisie. URL:http://dataportal.ins.tn/.

Kantoush, S.A., Schleiss, A.J., Sumi, T., Murasaki, M., 2011. Lspiv implementation for environmental flow in various laboratory and field cases. Journal of Hydro-environment Research 5 (4), 263–276. https://doi.org/10.1016/j.jher.2011.07.002.. URL:http://www.sciencedirect.com/science/article/pii/S1570644311000736 (iMAGE VELOCIMETRY).

Le Boursicaud, R., Pénard, L., Hauet, A., Thollet, F., Le Coz, J., 2016. Gauging extreme floods on youtube: application of lspiv to home movies for the post-event determination of stream discharges. Hydrological Processes 30 (1), 90–105. https://doi.org/10.1002/hyp.10532.

Le Coz, J., Patalano, A., Collins, D., Guillen, N.F., Garcia, C.M., Smart, G.M., Bind, J., Chiaverini, A., Le Boursicaud, R., Dramais, G., Braud, I., 2016. Crowdsourced data for flood hydrology: feedback from recent citizen science projects in Argentina, France and New Zealand. Journal of Hydrology 16 (2), 766–777. https://doi.org/10.1016/j.jhydrol.2016.07.036.

Leitão, J.P., Peña-Haro, S., Lüthi, B., Scheidegger, A., de Vitry, M.M., 2018. Urban overland runoff velocity measurement with consumer-grade surveillance cameras and surface structure image velocimetry. Journal of Hydrology 565, 791–804. https://doi.org/10.1016/j.jhydrol.2018.09.001.

Levene, H., 1960. Robust tests for equality of variances. Contributions to Probability and Statistics: Essays in Honor of Harold Hotelling 52 (3–4), 278–292.

Lüthi, B., Philippe, T., Peña-Haro, S., 2014. Mobile device app for small open-channel flow measurement. In: Smart and Mobile Devices Used for Environmental Applications. International Environmental Modelling and Software Society (iEMSs), San Diego, CA, USA, pp. 283–287. URL:http://www.iemss.org/society/index.php/iemss-2014-proceedings.

Lüthi B., Philippe T., Peña-Haro S., 2018. Method and system for determining the velocity of a moving fluid surface. Technical Report; Google Patents.

Miller, K.S., 1981. On the inverse of the sum of matrices. MathematicsMagazine 54 (2), 67–72.

Nezu, I., Sanjou, M., 2011. Piv and ptv measurements in hydro-sciences with focus on turbulent open-channel flows. Journal of Hydro-environment Research 5 (4), 215–230. https://doi.org/10.1016/j.jher.2011.05.004. (iMAGE VELOCIMETRY).

Paul, J.D., Buytaert, W., Allen, S., Ballesteros-Cánovas, J.A., Bhusal, J., Cieslik, K., Clark, J., Dugar, S., Hannah, D.M., Stoffel, M., Dewulf, A., Dhital, M.R., Liu, W., Nayaval, J.L., Neupane, B., Schiller, A., Smith, P.J., Supper, R., 2018. Citizen science for hydrological risk reduction and resilience building. WIREs Water 5 (1), e1262. https://doi.org/10.1002/wat2.1262.

Photrack, H., 2018. Discharge app. URL:https://discharge.ch.

Photrack, H., 2018. Global iMoMo Initiative. URL:https://www.imomohub.com/.

Pocock, M.J.O., Roy, H.E., August, T., Kuria, A., Barasa, F., Bett, J., Githiru, M., Kairo, J., Kimani, J., Kinuthia, W., Kissui, B., Madindou, I., Mbogo, K., Mirembe, J., Mugo, P., Muniale, F.M., Njoroge, P., Njuguna, E.G., Olendo, M.I., Opige, M., Otieno, T.O., Ng'weno, C.C., Pallangyo, E., Thenya, T., Wanjiru, A., Trevelyan, R., 2019. Developing the global potential of citizen science: Assessing opportunities that benefit people, society and the environment in east africa. Journal of Applied Ecology 56 (2), 274–281. https://doi.org/10.1111/1365-2664.13279.

Roy, H., Pocock,, M., Preston, C., Roy, D., Savage, J., Tweddle, J., Robinson, L., 2012. Understanding citizen science and environmental monitoring: final report on behalf of UK Environmental Observation Framework. Technical Report; Natural History Museum; Wallingford. URL:http://nora.nerc.ac.uk/id/eprint/20679/ (freely available online – click on Official URL link for full text).

See, L., 2019. A review of citizen science and crowdsourcing in applications of pluvial flooding. Frontiers in Earth Science 7, 44. https://doi.org/10.3389/feart.2019.00044.

Sellami, H., Vanclooster, M., Benabdallah, S., La Jeunesse, I., 2013. Assessment of the swat model prediction uncertainty using the glue approach a case study of the chiba catchment (tunisia). In: 2013 5th International Conference on Modeling, Simulation and Applied Optimization (ICMSAO), pp. 1–6. https://doi.org/10.1109/ICMSAO.2013.6552605.

Shapiro, S.S., Wilk, M.B., 1965. An analysis of variance test for normality (complete samples). Biometrika 52 (3–4), 591–611. https://doi.org/10.1093/biomet/52.3-4.591.

Tarpanelli, A., Brocca, L., Lacava, T., Faruolo, M., Melone, F., Moramarco, T., Pergola, N., Tramutoli, V., 2011. River discharge estimation through MODIS data. In: Neale C.M. U., Maltese A., (Eds.), Remote Sensing for Agriculture, Ecosystems, and Hydrology XIII. International Society for Optics and Photonics, SPIE, vol. 8174, pp. 77–84. doi:10.1117/12.898201.

Tauro, F., Selker, J., van de Giesen, N., Abrate, T., Uijlenhoet, R., Porfiri, M., Manfreda, S., Caylor, K., Moramarco, T., Benveniste, J., Ciraolo, G., Estes, L., Domeneghetti, A., Perks, M.T., Corbari, C., Rabiei, E., Ravazzani, G., Bogena, H., Harfouche, A., Brocca, L., Maltese, A., Wickert, A., Tarpanelli, A., Good, S., Alcala, J.M.L., Petroselli, A., Cudennec, C., Blume, T., Hut, R., Grimaldi, S., 2018. Measurements and observations in the xxi century (moxxi): innovation and multi-disciplinarity to sense the hydrological cycle. Hydrological Sciences Journal 63 (2), 169–196. https://doi.org/10.1080/02626667.2017.1420191.

Van Dijk, A.I.J.M., Brakenridge, G.R., Kettner, A.J., Beck, H.E., De Groeve, T., Schellekens, J., 2016. River gauging at global scale using optical and passive microwave remote sensing. Water Resources Research 52 (8), 6404–6418. https://doi.org/10.1002/2015WR018545.

Walker, D., Forsythe, N., Parkin, G., Gowing, J., 2016. Filling the observational void: scientific value and quantitative validation of hydrometeorological data from a community-based monitoring programme. Journal of Hydrology 538, 713–725. https://doi.org/10.1016/j.jhydrol.2016.04.062.